This document is the Accepted Manuscript version of a Published Work that appeared in final form in Sensors and Actuators B 226 (2016) 110–117. http://dx.doi.org/10.1016/j.snb.2015.11.109

NH_3 sensing with self-assembled ZnO-nanowire μHP sensors in isothermal and temperature-pulsed mode

F. Shao [a,b,*], J.D. Fan [a,c], F. Hernández-Ramírez [a,d,*], C. Fàbrega [a], T. Andreu [a], A. Cabot [a], J.D. Prades [d], N. López [e], F. Udrea [f,g], A. De Luca [f], S.Z. Ali [g], J.R. Morante [a,d]

[a] *Catalonia Institute for Energy Research (IREC), Sant Adrià del Besòs E-08930, Spain*
[b] *School of Electronic Science and Engineering, Nanjing University, Nanjing 210023, China*
[c] *Clarendon Laboratory, University of Oxford, Parks Road, Oxford OX1 3PU, United Kingdom*
[d] *Department of Electronic, University of Barcelona, Barcelona E-08028, Spain*
[e] *Institute of Chemical Research of Catalonia (ICIQ), Tarragona 43007, Spain*
[f] *Department of Engineering, University of Cambridge, Cambridge, United Kingdom*
[g] *Cambridge CMOS Sensors Ltd, Cambridge, United Kingdom*

A B S T R A C T

Dielectrophoretic alignment is found to be a simple and efficient method to deposit the solution prepared ZnO nanowires onto micro hot plate substrates. Due to the strong surface effects, positive temperature coefficient for resistance was encountered with ZnO nanowires in the high temperature range (>250 °C). The response to ammonia (NH_3) was evaluated in isothermal and temperature-pulsed operation mode; the relative higher response observed in the latter case demonstrates that the use of this methodology is a good strategy to improve the performance of metal oxide sensors based on nanomaterials. Here, we evaluate the response to NH_3 and qualitatively describe the sensing mechanism in temperature-pulsed mode, highlighting the main differences compared to the standard isothermal methodology.

Keywords:
ZnO
Nanowire
Micro hot plate
Ammonia
Gas sensor
Temperature-pulsed

1. Introduction

Silicon on insulator (SOI) [1] technology offers the possibility of fabricating mono-crystalline silicon electronics with good thermal isolation. Micro hot plates (μHPs) based on standard complementary metal oxide semiconductor (CMOS) processing technology [2] using tungsten (W) metallization [3] and/or the SOI layer for the micro-heater are an ideal choice of substrates for resistive metal oxides (MOX) gas sensors. In addition to the very low power consumption (tens of mW in DC operation) and fast thermal response (tens of ms) [3], they can be cost effectively manufactured in high volume and integrated with other functional electronics [4,5]. On top of the μHPs (above the micro-heater), inter digital electrodes (IDEs) are usually patterned to monitor the resistance variation in the sensing layer during the change of gas compositions at the elevated temperature. The size of the whole device is often mm × mm and the dimensions of the IDEs above the heater are of hundreds of micrometers. The miniaturization of the devices creates however a challenge, i.e., the deposition of sensing materials onto the micro-heater membrane in an effective way [6].

Conventional non-localized deposition techniques, e.g., sputtering [7–9], evaporation [10], spray coating [11] or electro-spinning [12] have to be combined with lithography of a deposition window or alignment of shadow masks; whereas localized deposition techniques that utilize the internal micro-heater to activate the growth have to use vapor phase precursors [6]. And if seed layers are required for the localized growth, the non-localized techniques are again needed to first produce them [13–15]. In the case of high precision screen printing [16], the deposition has to be made before the backside etching of the membrane to avoid its damage, making it inconvenient to the user of post CMOS wafer stage. Another set of techniques are those based on the direct deposition of sensing materials presented in liquid form by micro droplet coating [17,18] or ink-jet printing [19,20]. Apart from preparing the stable material suspension and the dedicated apparatuses, these two techniques also lack the capability of manipulating nanomaterials, e.g., the alignment of nanowires.

* Corresponding author.
E-mail addresses: fengangelo@hotmail.com (F. Shao), fhernandez@irec.cat (F. Hernández-Ramírez).

Dielectrophoretic (DEP) technique has been used to manipulate nanomaterials [21–24], especially metal [25] and semiconductor [23,26] nanowires. The DEP force arises from the polarization of non-charged elements in a non-uniform electric field and attracts the object to the electrodes. It has been successfully applied to align nanowires [25,27] or nanorods [28,29] onto different substrates for later sensing purposes, and it is suggested to be fully compatible with the standard CMOS technology for wafer-scale implementation [30,31].

MOXs are the most typical compounds studied and used as low cost resistive sensing materials. ZnO nanowires in particular have been identified as potential candidates to fabricate new devices [32]. Although ZnO nanowire-based gas sensors have been intensively studied in the last few years and promising results have been demonstrated [33–35], improvements are still needed to bring them into the commercial stage. On the other hand, μHP gas sensors are often investigated under the so-called temperature-programmed/modulated operation mode [36–40]. In this approach, the sensors are subjected to pulses of different temperatures and duration, instead of keeping the sensors' temperature at constant. Improvement of the sensors' selectivity and even quantification of gases [41,42] can be achieved by pattern reading and data analysis. A variant to that is the so called temperature-pulsed operation mode [18,41,43,44], in which the temperature of the sensor is constantly changed between two values (low and high) every few seconds and the resistance variation due to analyte gas at the low or high temperature end define the sensor response. With this approach, the sensitivity enhancement at the low temperature end is usually found.

In this work, the material deposition onto μHPs was further developed by applying the DEP alignment of ZnO nanowires at the post CMOS wafer stage. The gas sensing performance of the devices were tested with NH_3 in both conventional isothermal and temperature-pulsed sensing modes. The mechanism that lies behind the enhanced sensing performance in the temperature-pulsed mode is qualitatively discussed.

2. Experimental

2.1. Nanowire preparation

ZnO nanowires were obtained by a hydrothermal process reported earlier [45]. In brief, an 80 nm thick of ZnO seed layer were first sputtered onto indium doped tin oxide (ITO) glass. The ITO glass was then placed in the growth solution that consists of 0.02 M zinc nitrate, 0.015 M hexamethylenetetramine (HMTA), 0.004 M polyethyleneimine (end-capped, molecular weight 800 g/mol) and 0.024 M ammonium hydroxide. The solution was heated to 88 °C, and after 3 h, ZnO nanowires grew to about 6 μm in length with diameters range between 50 and 300 nm. The resulting ZnO arrays were rinsed with Milli-Q water and dried with nitrogen flow. More characterization results with, e.g., X-ray diffraction (XRD), scanning electron microscopy (SEM) can be found in ref.[45]. The solution of ZnO nanowires was obtained by sonicating the ITO substrate in isopropanol.

2.2. The μHPs

μHPs were obtained from Cambridge CMOS Sensors (www.ccmoss.com) [5]. The μHPs used in this work have IDEs made of gold (Au). Au is inert to oxidation and the rough Au surface provides good attachment to the later deposited nanowires. As shown in Fig. 1a, the IDEs span a circular area of 250 μm in diameter and the gap between the IDE fingers is 10 μm. The heating element made of W is buried under the IDEs within the SiO_2 insulation. W is used as an interconnect metal in high temperature CMOS processes and has better stability and lower mechanical stress compared to poly-Si heaters. The circular SiO_2 insulating membrane obtained by deep reactive ion etching (DRIE) has a diameter of 640 μm and a thickness of about 5 μm. Several Au bond pads that connect to the heater or IDEs are manufactured on the two sides of the chips for wire bonding. The maximum temperature the μHPs can reach is about 700 °C, while the power consumption is only about 55 mW at 450 °C.

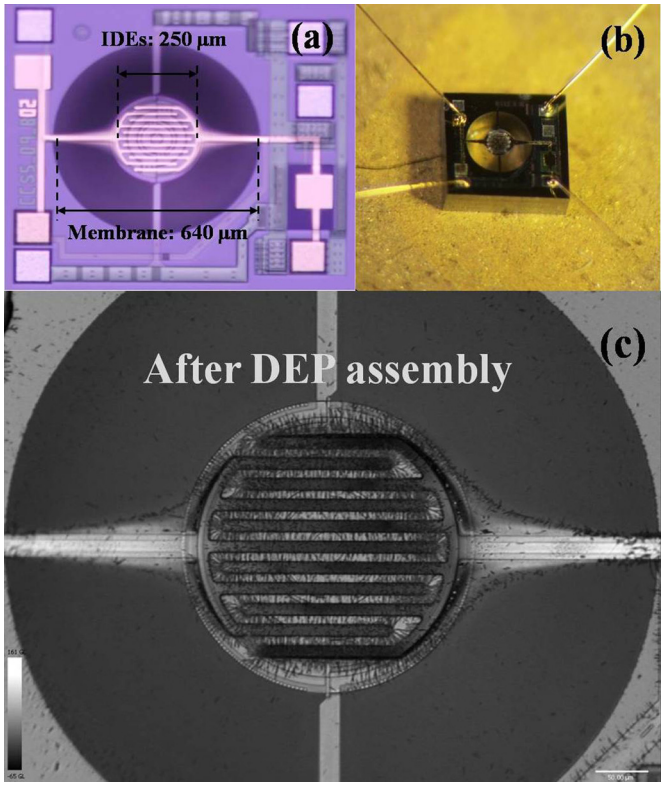

Fig. 1. (a) Layout of the CMOS SOI μHP substrate with gold IDEs. (b) The μHP substrate after wire bonding and nanowire deposition (ZnO nanowires appear in white under optical microscope). (c) Digital microscope image of the membrane after nanowire deposition (nanowires and IDEs both appear in deep color).

2.3. DEP assembly of nanowires

The μHP chips were glued onto the transistor outline packages (TO-8) and wire bonded with Au wires (Fig. S1). The devices were then attached to a printed circuit board for ZnO nanowire deposition and later tests. ZnO nanowire solution in isopropanol was briefly sonicated before use. A micropipette was used to apply 2 drops (~2.5 μl each) of it onto the μHPs when the AC potential was applied on the IDEs by a function generator (TG2000, TTi). The voltage applied was 15 V_{p-p} in square wave at the frequency of 5 MHz. Once the solvent had evaporated, the AC signal was turned off. The morphology of aligned nanowires on μHPs was examined using a SEM (Auriga, Zeiss). As the annealing/sintering step, the temperature of the μHPs was raised to 400 °C in stepwise and dwelled for 2 h.

2.4. Gas sensing tests

Gas sensing tests were performed with a homemade stainless steel chamber. Gas mixtures were introduced with thermal mass flow controllers (Bronkhost) by mixing the synthetic air (SA) with NH_3 in SA from the certified gas cylinders (Carburos Metálicos).

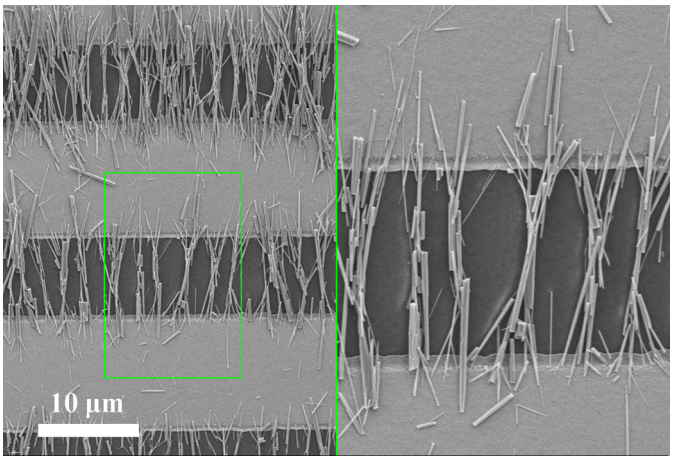

Fig. 2. SEM image showing nanowires assembled between the IDEs (the right half is the magnified image of the area in the small box on the left side).

The total flow rate was always maintained at 200 ml/min. The micro-heater was powered by a source meter (2400, Keithley). For temperature-pulsed measurement, the pulsed voltage was in square waves and has a period of 10 s, i.e., the temperature of sensor changed between the low and high regime every 5 s. The settle time of both rise and fall of the pulsed input voltage were measured to be within 50 ms. Electrical measurements were made with another source meter (2635A, Keithley).

3. Results and discussion

3.1. The assembled device

From the microscope images (Fig. 1b and c), we see that most of the nanowires were attached to the IDEs after the DEP process. The rest of the membrane surface was clean, and the small amount of nanowires left on the membrane presumably does not affect the overall performance of the device. As it is shown in Fig. 1c and Fig. S2, both the finger tips and the outmost of the IDEs had attracted the nanowires more efficiently compared to the center area. This result might arise from the interference presented at the center area when multiple IDEs fingers with an opposite potential were located very close to each other. The potential interference from nearby IDEs fingers can offset the polarization and attraction effects on the nanowires, leaving the center with fewer nanowires. SEM image in Fig. 2 shows that nanowires were aligned into bundles and interconnected to each other. Since their lengths are shorter than the gap between the IDEs, multiple nanowires are required to bridge the gap. Comparing to the nanowires that grow vertically on the membrane [13–15] and only having their bottom parts in contact with the membrane, the direct lying of nanowires on the μHP membrane offers better heat transfer property between the membrane and nanowires. This assures the annealing/sintering step can be used to strength the connections between the nanowires or nanowire-electrodes. The finally obtained structures were proved to be stable, since no direct evidence of degradation or change of their properties was found after regularly testing and handling. This suggests that the bond strength among nanowires and nanowire-electrodes are strong enough to fabricate functional devices following our approach.

3.2. Electrical properties

The contact between semiconductor and metal can be either ohmic or rectifying depending on whether a Schottky barrier is present. Ideally, ohmic contact is obtained with n-type

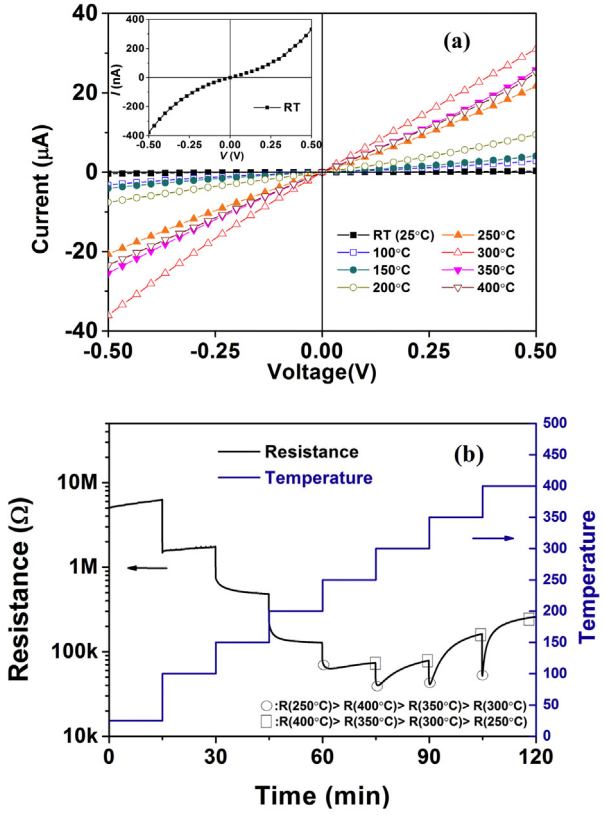

Fig. 3. (a) *I–V* curves of the annealed device at different temperatures, (inset) room temperature (RT) *I–V* curve. Note the measurements were made about 1–2 min after the temperature adjustment, the resistance order of $R(250\,^{\circ}C) > R(400\,^{\circ}C) > R(350\,^{\circ}C) > R(300\,^{\circ}C)$ can be retrieved. (b) Resistance variation with temperature increasing in steps (measured with probing current of 100 nA); ○: non-stabilized region, □: stabilized region.

semiconductor if the work function of the metal is close or smaller than the electron affinity of the semiconductor [46]. In our case, Au has a work function of 5.1 ± 0.1 eV [47] which is larger than the theoretical electron affinity of ZnO (~4.2 eV) [46]. The room temperature (RT) *I–V* curves (inset in Fig. 3a) of the annealed/sintered devices were found non-linear, indicating thus the formation of Schottky barrier at the Au–ZnO interface. The Schottky barrier however could be overcome by increasing the temperature [48]. The *I–V* curves became linear at 200 °C and above, so the contact resistance contribution can be neglected in the later gas sensing measurements at high temperature.

The current values in *I–V* tests were found to increase with temperature until 300 °C and then slightly declined at higher temperatures (Fig. 3a). These two opposite trends correspond to the negative (NTC) and positive temperature coefficients (PTC) of resistance, respectively. The negative one at low *T* results from the thermal generation of charge carriers and the overcoming of the Schottky and nanowire–nanowire junction barriers by electrons. On the other hand, the PTC after 300 °C resembles the results reported for ZnO thin films by Min et al. [9,49] and shows the same tendency as those reported for ZnO nanorods [50] and nanofibers [51] in a slightly varied temperature range. The resistance was further measured with increasing the temperature in steps (Fig. 3b). The resistance was found to decrease along with the temperature rise until 250 °C and only small drifts were observed during the dwell period. When the μHP temperature were raised to higher values, immediate drop of resistance were followed by drastic increase in the dwell period. The final resistance at 300 °C has surpassed 250 °C and even higher resistances were reached above this threshold. Such gradual increase of resistance also indicates that

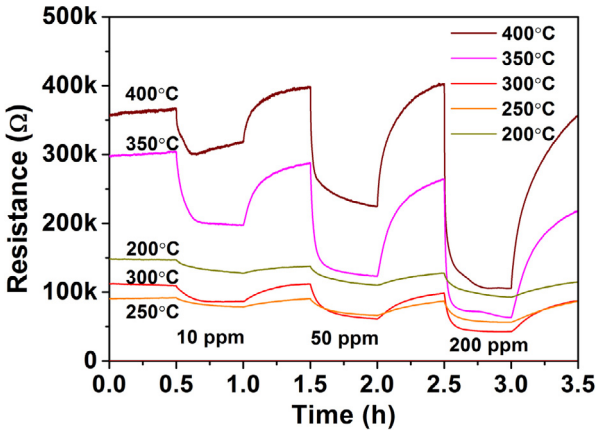

Fig. 4. NH_3 sensing of the ZnO nanowire device in isothermal mode.

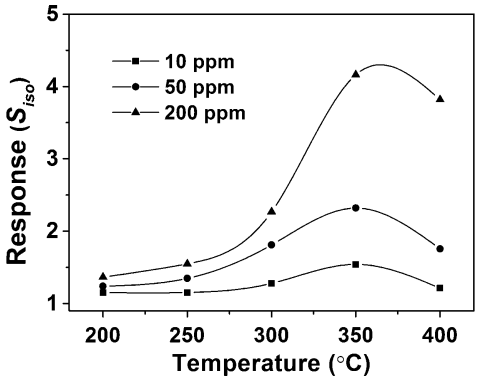

Fig. 5. Response vs. T of ZnO nanowires to different concentration of NH_3 in isothermal mode ($S_{iso} = R_{SA}/R_{gas}$).

the I–V measurements are dependent on both the temperature and the dwell time at that temperature. As the I–V results in Fig. 3a were obtained about 1–2 min after the temperature adjustment, it follows the order of $R(250\,^{\circ}C) > R(400\,^{\circ}C) > R(350\,^{\circ}C) > R(300\,^{\circ}C)$, which is consistent with Fig. 3b only in the non-stabilized region right after the temperature change (marked with circles in Fig. 3b). Moreover, the more stabilized region in Fig. 3b with $R(400\,^{\circ}C) > R(350\,^{\circ}C) > R(300\,^{\circ}C) > R(250\,^{\circ}C)$ is consistent with Fig. 4 in the next section.

Regarding the origin of the PTC phenomenon, we first exclude the possibility of bulk chemical structure or composition change as the nanowires were pre-annealed and had experienced long hours of repeated gas sensing tests at high temperatures, in which we have seen a stabilized resistance base line. Furthermore, the nanowire-electrode contacts were shown to be ohmic at the elevated temperatures, making no contribution to the measured resistance. ZnO nanowires studied here also do not satisfy the two well-known PTC effects caused by interfaces: the PTC effect in ferroelectric ceramic materials [52] and the PTC effect in composite oxides materials [53]. On the other hand, due to the strong surface dependence of nanomaterials, the cause of the PTC in MOX nanomaterials has been ascribed to the complex dynamics of thermal desorption of water and related hydroxyl group (—OH) or generation of charged atomic O species (O^-/O^{2-}) on the surface [9,49–51,54,55]. For oxygen, the adsorbed molecular O_2^- dissociate in to O^- and O^{2-} at high temperatures, which apparently withdraw the electron more efficiently. And for the chemisorbed H_2O and its by-product —OH, they act as the electron donor to the oxides, lowering the resistance at low temperature and increasing the resistance when removed by high temperature. Considering the high defect density of the solution prepared ZnO nanowires, the defects may have strong influence on their properties and have deeply involved in the as mentioned surface chemistries. Nevertheless, as will be shown next, despite the presence of the PTC, it does not undermine the capability of ZnO nanowires for gas sensing.

3.3. NH_3 sensing

NH_3 sensing tests were first performed at temperatures between 200 °C and 400 °C in the isothermal mode. As shown in Fig. 4, the response baseline in SA was fixed after the complete stabilization of the electrical resistance following a change in T. For this reason and in agreement with the abovementioned positive temperature coefficient of the devices, the initial resistance was found to slightly increase from 300 °C and above. In all cases, nanowires responded to NH_3 by decreasing the resistance and the change was reversible when NH_3 was purged from the chamber. The decrease of the resistance upon exposure to NH_3 was expected as ZnO is an n-type semiconductor and NH_3 is a reducing gas. Here we define the isothermal mode response S_{iso} to be R_{SA}/R_{gas}, where R_{SA} and R_{gas} are the resistance values in SA and in gas mixture, respectively. Response and recovery time (t_{res} and t_{rev}) were counted as the time it took to complete 90% of the total resistance change. The optimal working temperature for NH_3 ($S_{iso} = 4.2$ for 200 ppm; 2.3 for 50 ppm and 1.5 for 10 ppm) was found to be 350 °C (Fig. 5). At this temperature, t_{res} were 7.4, 6.4 and 3.8 min for 10, 50 and 200 ppm of NH_3, and the corresponding t_{rev} were 18.4, 19.9 and 21.5 min, respectively. All these values are however convoluted with the dynamics of the chamber.

A survey of literature reported resistive nano-sensors is given in Table S1 of the supplementary material. The S_{iso} value here obtained is found comparable to other studies of similar materials [56–58]. Indeed, the dependence of the gas response with the nanowires diameter is a well-known effect [35]; the response clearly benefits from the smaller diameters. This is more significant with thickness approaching to the Debye length. Herein, ZnO nanowires with diameters between 50 and 300 nm were tested and the thicker nanowires are believed to be the major current pathway. So the nanowires diameter is not favored by the high response and improvement can be simply made by making more uniform and thinner nanowires.

The NH_3 response of ZnO nanowires can be explained using the classic model [59] of MOX gas sensors: the surface oxygen species (molecular O_2^- and atomic O^-, O^{2-}) withdraw electrons from the ZnO, creating a depletion region that acts as a non-conductive region at the surface and charge transfer barrier between the nanowire junctions (as shown in Fig. 6). When the NH_3 is present, surface reaction occurs between the surface oxygen species and the adsorbed NH_3 molecule. These complex surface reactions can be simply described by the following equation [60]:

$$O_2^-/O^-/O^{2-} + NH_3(ad) \leftrightarrow Nspecies + H_2O + e^-$$

With N_2 as the main reaction product, electrons are released by the surface reactions and the resistance of ZnO decreases. In more specific, ohmic contacts formation was previously confirmed between nanowires and electrodes at the elevated temperatures. So the measured resistance is composed of the resistance of nanowire themselves ($R_{nanowire}$) and the resistance at nanowire–nanowire junctions ($R_{junction}$). As illustrated in Fig. 6, the surface reactions release the electrons back into the nanowires, causing the reduction of depletion region width and lowering of junction potential barriers. The two contributors of the total resistance, $R_{nanowire}$ and $R_{junction}$ are therefore both lowered and finally lead to the reduction of the measured resistance.

In Fig. 4, it can be noted that the resistance indeed showed upward shifting after a prior drop at the 10 ppm response of 400 °C. And the recovered resistance after 10, 50 ppm exposure exceeded

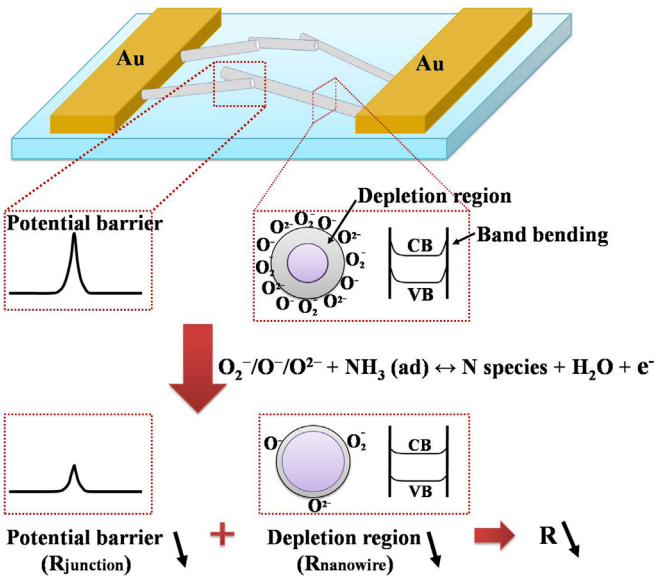

Fig. 6. Schematic illustrating the mechanism of NH_3 sensing.

the base value. Such character could be ascribed to the generation of NO_2 in addition to N_2 by the surface reactions; as NO_2 is considered to get adsorbed on the surface and withdraws electron [40,61,62]. The reason it appeared only at the low NH_3 level and highest temperature might be the request on high energy and selectively producing of NO_2 [57]. Moreover, the counter-balancing effect of NH_3 might also cause it to be more visible at the low NH_3. All in all, the ammonia response follows a typical bell-shaped curve (Fig. 5), which reveal that ammonia sensing is (i) a thermally activated process but also that (ii) the response (reaction rate) is given by the ammonia adsorption-reaction probabilities at the surface, following a non-linear dependence of the sensor output with increasing concentration. Actually, this behavior was explained by Ahlers et al. [63] in terms of competing phenomena described by two energetic parameters: the strength of Langmuir adsorption E_{ads} of NH_3 molecules at the surface, and the activation energy for the combustion reaction E_{RES}. These two factors are thus the decisive parameters to explain the high-temperature drop-off of the sensitivity S. It must be pointed out that between 350 °C and 400 °C the response starts to decrease.

In the temperature-pulsed mode, the sensor temperature was continuously changed between a low (200 °C or 250 °C) and a higher value for every 5 s. The resistance of the nanowires was simultaneously recorded when the gas flow was switched from pure SA to 200 ppm NH_3 in SA and then purged back to SA. The resistance in the low temperature end was used to calculate the corresponding response $S_{pulsed,low}$. As shown in Fig. 7, when the sensors were operated in the temperature-pulsed mode, the low or high end resistance no more equals to that in the isothermal mode of same temperature. And only the negative temperature

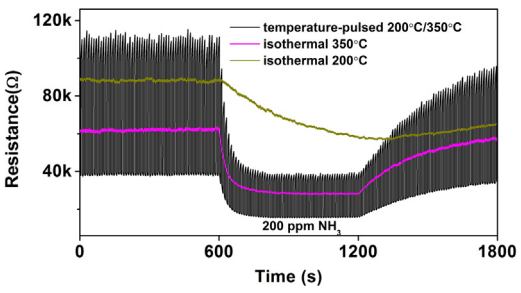

Fig. 7. Temperature-pulsed and isothermal sensing of 200 ppm NH_3.

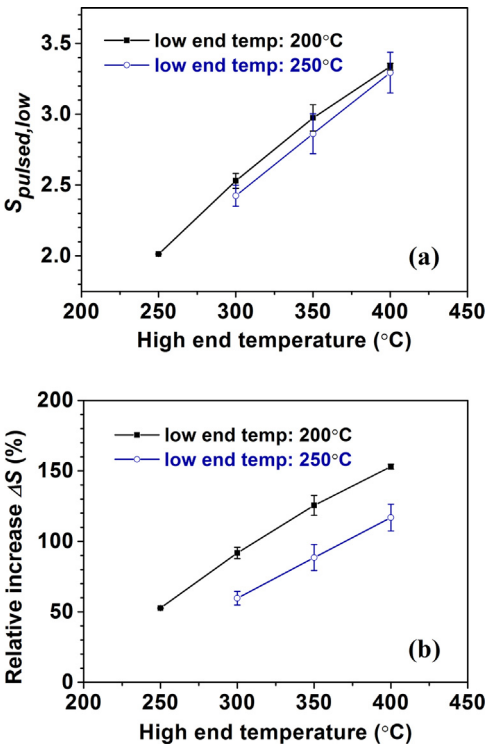

Fig. 8. (a) Response $S_{pulsed,low}$ for low end temperature of 200 and 250 °C. (b) Relative response increase ΔS. The error bars represent the sample standard deviation of 3 measurements.

coefficient was observed when changing the temperature in short pulses. A significant enhancement of response $S_{pulsed,low}$ compared to the isothermal mode of same temperature was observed. For 200 °C or 250 °C as the low end temperature, the response $S_{pulsed,low}$ increased with the high end temperature following a linear dependence (Fig. 8a). And the response $S_{pulsed,low}$ of a particular high end temperature were highly approximate to each other. This indicates that in this mode, $S_{pulsed,low}$ is determined by the high end temperature. The relative response compared to that of the isothermal mode was calculated as $\Delta S = (S_{pulsed,low} - S_{iso,low})/S_{iso,low} \times 100\%$ and given in Fig. 8b. Here, $S_{iso,low}$ is the isothermal response in the corresponding temperature. From the tests, ΔS with 200 °C as the low end temperature were found to be always higher than that of 250 °C, indicating that ΔS also increases with the difference between the high and the low end temperatures. Although strongly affected by the chamber volume and the gas flow rate, the response and recovery of the resistance also became faster in the pulsed mode (see Fig. S3). Overall, the low temperature end t_{res} at the pulsed mode decreased with increasing high end temperature and the values are about on a par with that of the isothermal mode in the temperature same to the high end. An equivalent correlation was found for the recovery. Due to the fact that resistance did not recover completely within the given time (10 min), the recovery ratio ($R_{end}/R_{SA} \times 100\%$, where R_{end} is the resistance when ending the SA refill) is defined. With pulsed temperature (especially at 300 °C and 350 °C high end T), the recovery ratio of the pulsed mode increased to higher values.

Similar response enhancement effects in the temperature-pulsed mode operation of μHP gas sensors have been previously reported in several works [18,41,43,44]. As the surface oxygen species play a key role in the sensing mechanisms of reducing gases, A. Heilig et al. [41], proposed that the enhancement is mainly caused by the presence of high temperature surface oxygen species, i.e., O^-/O^{2-} [59] in the low temperature period, which would be less or not existed in the equivalent isothermal mode. O^-/O^{2-} are produced after the dissociation [64] of surface adsorbed molecular

oxygen at high temperatures and remains there in the low temperature period due to the fast thermal transition of this mode. They strongly regulate the electron concentration near the surface and when surface reaction with reducing gas occurs, electrons will be released back to the surface to cause the resistance change. Furthermore, the higher reactivity of atomic O^-/O^{2-} with NH_3 will also lead to the faster response and recovery processes.

As mentioned in Refs. [18,39], the surface cleaning effect during the high temperature period could also be the reason behind the response enhancement. Here, for the NH_3 sensing with ZnO nanowires, we propose two potential adsorbates that can deteriorate the performance of the sensor in isothermal mode and can be removed at high temperatures. The first is H_2O and its by product, hydroxyl group (—OH). H_2O is a well-known substance that interferes the output of MOX gas sensors [65,66]. H_2O and its byproduct —OH has been appointed as one of the causes of positive temperature coefficient in the previous section. There are three sources of H_2O that can be adsorbed onto ZnO surface: (i) when the sensor is exposed to ambient air at RT; (ii) the trace level of H_2O presented in the SA; (iii) the residual H_2O in the test chamber. The second adsorbate is NO_2, which was considered to be a secondary product of oxygen-NH_3 reaction at the surface and has a counter effect on NH_3 sensing [40,61,62]. When operated in the temperature-pulsed mode, the amount of H_2O/—OH and NO_2 can be diminished during the high temperature period. Exposing the free surface active sites to O_2 and NH_3 at low temperature period will enable a higher response and faster surface sensing mechanisms. Fig. S4 shows, in a shorter time scale, the resistance of the device working in temperature-pulsed mode between 200 and 350 °C in constant SA flow. As expected, the resistance was found to drift continuously in both high and low temperature period after a sudden large change due to the fast temperature switch. This indicates the material was in a meta-stable state, which is evidence to the as proposed sensing mechanism and the response enhancement.

4. Conclusions

ZnO nanowires were successfully deposited onto CMOS SOI μHP substrates for gas sensing applications. By DEP, nanowires prepared from a wide range of methods can be readily integrated onto μHPs. When working in the pulsed mode, a significant enhancement in the NH_3 sensing performance was observed at the low temperature end. It is proposed that this phenomenon is not only related to the high temperature surface oxygen species but also to the modulation of H_2O (—OH) and N_2O on the surface. The combination of the highly advanced CMOS SOI μHPs with this operation mode provides a new option to obtain reliable low cost gas sensors with even lower power consumption and high response.

Acknowledgements

The research was supported by the Framework 7 program under the project SOI-HIT (FP7-FP7-ICT-2011-7) and European Regional Development Funds (ERDF). Authors from IREC acknowledge the financial support given by the XaRMAE Network of Excellence on Materials for Energy of the "Generalitat de Catalunya". F.H.-R. also acknowledges the support of the DAAD (D/11/43761). J. Fan also thanks for the support of the Secretary for Universities and Research of the Ministry of Economy and Knowledge of the Government of Catalonia.

Appendix A. Supplementary data

Supplementary data associated with this article can be found, in the online version, at http://dx.doi.org/10.1016/j.snb.2015.11.109.

References

[1] T. Iwaki, J.A. Covington, J.W. Gardner, F. Udrea, C.S. Blackman, I.P. Parkin, SOI-CMOS based single crystal silicon micro-heaters for gas sensors, in: 2006 IEEE Sensors, 2007, pp. 460–463.
[2] O. Brand, G.K. Fedder, CMOS-MEMS, Wiley-VCH, 2005.
[3] S.Z. Ali, F. Udrea, W.I. Milne, J.W. Gardner, Tungsten-based SOI microhotplates for smart gas sensors, J. Microelectromech. Syst. 17 (2008) 1408–1417.
[4] D. Barrettino, M. Graf, M. Zimmermann, C. Hagleitner, A. Hierlemann, H. Baltes, A smart single-chip micro-hotplate-based gas sensor system in CMOS-technology, Analog Integr. Circuits Signal Process. 39 (2004) 275–287.
[5] A. De Luca, V. Pathirana, S.Z. Ali, D. Dragomirescu, F. Udrea, Experimental, analytical and numerical investigation of non-linearity of SOI diode temperature sensors at extreme temperatures, Sens. Actuators A: Phys. 222 (2015) 31–38.
[6] S. Semancik, R.E. Cavicchi, M.C. Wheeler, J.E. Tiffany, G.E. Poirier, R.M. Walton, et al., Microhotplate platforms for chemical sensor research, Sens. Actuators B: Chem. 77 (2001) 579–591.
[7] J. Wöllenstein, J.A. Plaza, C. Cané, Y. Min, H. Böttner, H.L. Tuller, A novel single chip thin film metal oxide array, Sens. Actuators B: Chem. 93 (2003) 350–355.
[8] M. Stankova, X. Vilanova, J. Calderer, E. Llobet, J. Brezmes, I. Gràcia, et al., Sensitivity and selectivity improvement of rf sputtered WO_3 microhotplate gas sensors, Sens. Actuators B: Chem. 113 (2006) 241–248.
[9] Y. Min, H.L. Tuller, S. Palzer, J. Wöllenstein, H. Böttner, Gas response of reactively sputtered ZnO films on Si-based micro-array, Sens. Actuators B: Chem. 93 (2003) 435–441.
[10] A. Friedberger, P. Kreisl, E. Rose, G. Müller, G. Kühner, J. Wöllenstein, et al., Micromechanical fabrication of robust low-power metal oxide gas sensors, Sens. Actuators B: Chem. 93 (2003) 345–349.
[11] I. Jiménez, A. Cirera, A. Cornet, J.R. Morante, I. Gracia, C. Cané, Pulverisation method for active layer coating on microsystems, Sens. Actuators B: Chem. 84 (2002) 78–82.
[12] Y. Zhao, X. He, J. Li, X. Gao, J. Jia, Porous CuO/SnO_2 composite nanofibers fabricated by electrospinning and their H_2S sensing properties, Sens. Actuators B: Chem. 165 (2012) 82–87.
[13] S. Santra, S.Z. Ali, P.K. Guha, G.F. Zhong, J. Robertson, J.A. Covington, et al., Post-CMOS wafer level growth of carbon nanotubes for low-cost microsensors – a proof of concept, Nanotechnology 21 (2010) 485301.
[14] S. Barth, R. Jimenez-Diaz, J. Sama, J. Daniel Prades, I. Gracia, J. Santander, et al., Localized growth and in situ integration of nanowires for device applications, Chem. Commun. 48 (2012) 4734–4736.
[15] S. Santra, P.K. Guha, S.Z. Ali, P. Hiralal, H.E. Unalan, J.A. Covington, et al., ZnO nanowires grown on SOI CMOS substrate for ethanol sensing, Sens. Actuators B: Chem. 146 (2010) 559–565.
[16] E. Llobet, P. Ivanov, X. Vilanova, J. Brezmes, J. Hubalek, K. Malysz, et al., Screen-printed nanoparticle tin oxide films for high-yield sensor microsystems, Sens. Actuators B: Chem. 96 (2003) 94–104.
[17] J. Puigcorbé, A. Cirera, J. Cerdà, J. Folch, A. Cornet, J.R. Morante, Microdeposition of microwave obtained nanoscaled SnO_2 powders for gas sensing microsystems, Sens. Actuators B: Chem. 84 (2002) 60–65.
[18] A.M. Ruiz, X. Illa, R. Díaz, A. Romano-Rodríguez, J.R. Morante, Analyses of the ammonia response of integrated gas sensors working in pulsed mode, Sens. Actuators B: Chem. 118 (2006) 318–322.
[19] M.A. Andio, P.N. Browning, P.A. Morris, S.A. Akbar, Comparison of gas sensor performance of SnO_2 nano-structures on microhotplate platforms, Sens. Actuators B: Chem. 165 (2012) 13–18.
[20] J. Kukkola, M. Mohl, A.-R. Leino, G. Toth, M.-C. Wu, A. Shchukarev, et al., Inkjet-printed gas sensors: metal decorated WO_3 nanoparticles and their gas sensing properties, J. Mater. Chem. 22 (2012) 17878–17886.
[21] H.Y. Yu, B.H. Kang, U.H. Pi, C.W. Park, S.-Y. Choi, G.T. Kim, V_2O_5 nanowire-based nanoelectronic devices for helium detection, Appl. Phys. Lett. 86 (2005) 253102–253103.
[22] A.W. Maijenburg, M.G. Maas, E.J.B. Rodijk, W. Ahmed, E.S. Kooij, E.T. Carlen, et al., Dielectrophoretic alignment of metal and metal oxide nanowires and nanotubes: a universal set of parameters for bridging prepatterned microelectrodes, J. Colloid Interface Sci. 355 (2011) 486–493.
[23] C.S. Lao, J. Liu, P. Gao, L. Zhang, D. Davidovic, R. Tummala, et al., ZnO nanobelt/nanowire Schottky diodes formed by dielectrophoresis alignment across Au electrodes, Nano Lett. 6 (2006) 263–266.
[24] E.M. Freer, O. Grachev, X. Duan, S. Martin, D.P. Stumbo, High-yield self-limiting single-nanowire assembly with dielectrophoresis, Nat Nano 5 (2010) 525–530.
[25] X. Li, Y. Wang, Y. Lei, Z. Gu, Highly sensitive H_2S sensor based on template-synthesized CuO nanowires, RSC Adv. 2 (2012) 2302–2307.
[26] C. Leiterer, G. Broenstrup, N. Jahr, M. Urban, C. Arnold, S. Christiansen, et al., Applying contact to individual silicon nanowires using a dielectrophoresis (DEP)-based technique, J. Nanopart. Res. 15 (2013) 1–7.
[27] X. Li, Z. Gu, J. Cho, H. Sun, P. Kurup, Tin–copper mixed metal oxide nanowires: synthesis and sensor response to chemical vapors, Sens. Actuators B: Chem. 158 (2011) 199–207.
[28] W.J. Liu, J. Zhang, L.J. Wan, K.W. Jiang, B.R. Tao, H.L. Li, et al., Dielectrophoretic manipulation of nano-materials and its application to micro/nano-sensors, Sens. Actuators B: Chem. 133 (2008) 664–670.
[29] S.R. Mahmoodi, B. Raissi, E. Marzbanrad, N. Shojayi, A. Aghaei, C. Zamani, Dielectrophoretic assembly of ZnO nanorods for gas sensing, Proc. Chem. 1 (2009) 947–950.

[30] A.H. Monica, S.J. Papadakis, R. Osiander, M. Paranjape, Wafer-level assembly of carbon nanotube networks using dielectrophoresis, Nanotechnology 19 (2008) 085303.
[31] S. Evoy, N. DiLello, V. Deshpande, A. Narayanan, H. Liu, M. Riegelman, et al., Dielectrophoretic assembly and integration of nanowire devices with functional CMOS operating circuitry, Microelectron. Eng. 75 (2004) 31–42.
[32] U. Ozgur, D. Hofstetter, H. Morkoc, ZnO devices and applications: a review of current status and future prospects, Proc. IEEE 98 (2010) 1255–1268.
[33] Z. Fan, J.G. Lu, Gate-refreshable nanowire chemical sensors, Appl. Phys. Lett. 86 (2005).
[34] M.W. Ahn, K.S. Park, J.H. Heo, D.W. Kim, K.J. Choi, J.G. Park, On-chip fabrication of ZnO-nanowire gas sensor with high gas sensitivity, Sens. Actuators B: Chem. 138 (2009) 168–173.
[35] O. Lupan, V.V. Ursaki, G. Chai, L. Chow, G.A. Emelchenko, I.M. Tiginyanu, et al., Selective hydrogen gas nanosensor using individual ZnO nanowire with fast response at room temperature, Sens. Actuators B: Chem. 144 (2010) 56–66.
[36] R.E. Cavicchi, J.S. Suehle, K.G. Kreider, M. Gaitan, P. Chaparala, Fast temperature programmed sensing for micro-hotplate gas sensors, IEEE Electron Device Lett. 16 (1995) 286–288.
[37] K.D. Benkstein, B. Raman, D.L. Lahr, J.E. Bonevich, S. Semancik, Inducing analytical orthogonality in tungsten oxide-based microsensors using materials structure and dynamic temperature control, Sens. Actuators B: Chem. 137 (2009) 48–55.
[38] D.C. Meier, J.K. Evju, Z. Boger, B. Raman, K.D. Benkstein, C.J. Martinez, et al., The potential for and challenges of detecting chemical hazards with temperature-programmed microsensors, Sens. Actuators B: Chem. 121 (2007) 282–294.
[39] A.P. Lee, B.J. Reedy, Temperature modulation in semiconductor gas sensing, Sens. Actuators B: Chem. 60 (1999) 35–42.
[40] C. Bur, P. Reimann, A. Schutze, M. Andersson, A.L. Spetz, Increasing the selectivity of Pt-gate SiC field effect gas sensors by dynamic temperature modulation, in: Sensors IEEE2010, 2010, pp. 1267–1272.
[41] A. Heilig, N. Bârsan, U. Weimar, M. Schweizer-Berberich, J.W. Gardner, W. Göpel, Gas identification by modulating temperatures of SnO_2-based thick film sensors, Sens. Actuators B: Chem. 43 (1997) 45–51.
[42] R. Gosangi, R. Gutierrez-Osuna, Active temperature modulation of metal-oxide sensors for quantitative analysis of gas mixtures, Sens. Actuators B: Chem. 185 (2013) 201–210.
[43] M. Jaegle, J. Wöllenstein, T. Meisinger, H. Böttner, G. Müller, T. Becker, et al., Micromachined thin film SnO_2 gas sensors in temperature-pulsed operation mode, Sens. Actuators B: Chem. 57 (1999) 130–134.
[44] M. Schweizer-Berberich, S. Strathmann, U. Weimar, R. Sharma, A. Seube, A. Peyre-Lavigne, et al., Strategies to avoid VOC cross-sensitivity of SnO_2-based CO sensors, Sens. Actuators B: Chem. 58 (1999) 318–324.
[45] J. Fan, Y. Hao, A. Cabot, E.M.J. Johansson, G. Boschloo, A. Hagfeldt, Cobalt(II/III) redox electrolyte in ZnO nanowire-based dye-sensitized solar cells, ACS Appl. Mater. Interfaces 5 (2013) 1902–1906.
[46] L.J. Brillson, Y. Lu, ZnO Schottky barriers and Ohmic contacts, J. Appl. Phys. 109 (2011) 121301–121333.
[47] D.E. Eastman, Photoelectric work functions of transition, rare-earth, and noble metals, Phys. Rev. B 2 (1970) 1–2.
[48] F. Hernandez-Ramirez, A. Tarancon, O. Casals, E. Pellicer, J. Rodriguez, A. Romano-Rodriguez, et al., Electrical properties of individual tin oxide nanowires contacted to platinum electrodes, Phys. Rev. B 76 (2007) 085429.
[49] Y. Ming, Properties and Sensor Performance of Zinc Oxide Thin Films, Massachusetts Institute of Technology, 2003.
[50] H. Guan-nan, H. Bo, S. Hui, Positive temperature coefficient of resistance of single ZnO nanorods, Nanotechnology 22 (2011) 065304.
[51] S. Wei, S. Wang, Y. Zhang, M. Zhou, Different morphologies of ZnO and their ethanol sensing property, Sens. Actuators B: Chem. 192 (2014) 480–487.
[52] X.-w. Zhu, S.-w. Wang, S.-w. Zhong, Y.-y. Liu, S.-y. Shen, W.-z. Jiang, et al., PTCR effects in Sr-doped $KNbO_3$ ferroelectric ceramic materials, Ceram. Int. 40 (2014) 12383–12386.
[53] D. Lisjak, M. Drofenik, D. Kolar, Composite ceramics with a positive temperature coefficient of electrical resistivity effect, J. Mater. Res. 15 (2000) 417–428.
[54] G. Neri, A. Bonavita, G. Micali, G. Rizzo, N. Pinna, M. Niederberger, In_2O_3 and Pt-In_2O_3 nanopowders for low temperature oxygen sensors, Sens. Actuators B: Chem. 127 (2007) 455–462.
[55] X. Li, E. Chin, H. Sun, P. Kurup, Z. Gu, Fabrication and integration of metal oxide nanowire sensors using dielectrophoretic assembly and improved post-assembly processing, Sens. Actuators B: Chem. 148 (2010) 404–412.
[56] S.J. Chang, W.Y. Weng, C.L. Hsu, T.J. Hsueh, High sensitivity of a ZnO nanowire-based ammonia gas sensor with Pt nano-particles, Nano Commun. Netw. 1 (2010) 283–288.
[57] Q. Qi, T. Zhang, L. Liu, X. Zheng, G. Lu, Improved NH_3, C_2H_5OH, and CH_3COCH_3 sensing properties of SnO_2 nanofibers by adding block copolymer P123, Sens. Actuators B: Chem. 141 (2009) 174–178.
[58] C. Li, D. Zhang, B. Lei, S. Han, X. Liu, C. Zhou, Surface treatment and doping dependence of In_2O_3 nanowires as ammonia sensors, J. Phys. Chem. B 107 (2003) 12451–12455.
[59] N. Barsan, U. Weimar, Conduction model of metal oxide gas sensors, J. Electroceram. 7 (2001) 143–167.
[60] F. Shao, M.W.G. Hoffmann, J.D. Prades, J.R. Morante, N. López, F. Hernández-Ramírez, Interaction mechanisms of ammonia and tin oxide: a combined analysis using single nanowire devices and DFT calculations, J. Phys. Chem. C 117 (2013) 3520–3526.
[61] I. Jimenez, M.A. Centeno, R. Scotti, F. Morazzoni, A. cornet, NH_3 interaction with catalytically modified nano WO_3 powders for gas sensing applications, J. Electrochem. Soc. 150 (2003) 72–80.
[62] Y. Shimizu, T. Okamoto, Y. Takao, M. Egashira, Desorption behavior of ammonia from TiO_2 based specimens – ammonia sensing mechanism of double layer sensors with TiO_2 based catalyst layers, J. Mol. Catal. A: Chem. 155 (2000) 183–191.
[63] S. Ahlers, G. Müller, T. Doll, A rate equation approach to the gas sensitivity of thin film metal oxide materials, Sens. Actuators B: Chem. 107 (2005) 587–599.
[64] J. Oviedo, M.J. Gillan, First-principles study of the interaction of oxygen with the SnO_2 (110) surface, Surf. Sci. (2001) 221–236.
[65] F.H. Ramirez, S. Barth, A. Taracon, O. Casals, E. Pellicer, J. Rodriguez, et al., Water vapor detection with individual tin oxide nanowires, Nanotechnology 18 (2007) 424016.
[66] C.S. Rout, M. Hegde, A. Govindaraj, C.N.R. Rao, Ammonia sensors based on metal oxide nanostructures, Nanotechnology 18 (2007) 205504.

Biographies

Feng Shao graduated from Nanjing University of Aeronautics and Astronautics in 2006 and obtained an Msc degree from KTH Sweden in 2010. Then he conducted his research on nanowire gas sensors at Catalonia Institute for Energy Research and obtained his doctorate degree from the University of Barcelona in 2014. He is currently a postdoc at School of Electronic Science and Engineering, Nanjing University.

Jian Dong Fan conducted his doctoral research at Catalonia Institute for Energy Research obtained his doctorate degree from the University of Barcelona in 2013. He has focused his research on metal oxide nanowries/nanotube based dye solar cells. He is currently a Postdoctal researcher in Oxford University for perovskite solar cells.

Francisco Hernández-Ramírez graduated in Physics at the University of Barcelona in 2003 and obtained his Ph.D. at the same institution in 2007. He is actively involved in the development of innovative sensor prototypes based on nanowires. He has published more than 30 papers in peer-reviewed journals and contributed to five industrial patents.

Cristian Fàbrega obtained his PhD (2011) from University of Barcelona, devoted to the synthesis of titanium dioxide with nanostructured properties and their optical, electrical and electrochemical characterization for the generation of solar hydrogen using photoelectrochemical cells. He is physicist and has a strong background on different characterization techniques such as Atomic Force Microscope, X-ray Photoelectron Spectroscopy, Electron Paramagnetic Resonance, Photoluminescence and Impedance Spectroscopy.

Teresa Andreu received her degree in chemistry at the University of Barcelona in 1999 and the PhD in 2004 in Material Science. From 2004 to 2006, she worked in the R&D Department of MacDermid Inc. involved in plating on plastics and electroless deposition of nickel. In 2007, she joined the Electronics Department of the University of Barcelona, mainly focused on the synthesis of metal oxides using nanotemplates. Since 2009, she is a researcher of the Advanced Materials Area of IREC. Her current interests include synthesis and characterization of semiconductors and its application to chemical sensors, photocatalysis and electrocatalysis.

Andreu Cabot was born in 1976 in Barcelona. He graduated in Physics in 1998 and received his PhD in 2003 (University of Barcelona). He did postdoctoral research at the University of California, Berkeley, under Prof. A. Paul Alivisatos' guidance. He returned to the Electronics Department, University of Barcelona in 2007 and joined the Catalonia Institute for Energy Research (IREC) in 2009 to form the Functional Nanomaterials Group. His research interests include the preparation, characterization and assembly of metal and semiconductor nanocrystals, to increase the efficiency and reduce the cost of current systems for energy conversion and storage.

Joan D. Prades was born in Barcelona in 1982. He graduated in Physics at the University of Barcelona in 2005 and obtained his Ph.D. at the same institution in 2009. He has experience in modeling of the electronic and vibrational properties of nanostructured metal oxides and in their experimental validation. He is actively involved in the development of innovative device prototypes based on nanowires. He has published more than 40 papers in peer-reviewed journals and contributed to more than 10 international conferences. He has also contributed to five industrial patents.

Nuria López (Barcelona, 1972) graduated in Chemistry with honors at the University of Barcelona, Spain (1995) and got her PhD degree in Theoretical Chemistry "cum laude" at the same university (1999), in the group of Prof. F. Illas. She then moved to the Center for Atomic-scale Materials Physics for her post-doc in the group of Prof. Jens K. Nørskov (Denmark). In 2001 she moved back to the University of Barcelona as a *Ramón y Cajal* fellow. In 2004 she was appointed Distinguished Professor by the DURSI in the junior category (under 41 years old). In November 2005 she took a position at ICIQ, where she currently leads a research group with focus on the theoretical research heterogeneous catalysis. She is also a part-time professor at the Department of Physical Chemistry of the URV. Núria has co-authored over 70 scientific publications. In September 2010 her "Tenure Track" period was successfully evaluated by an experts committee and she became a "Senior Group Leader" at ICIQ.

Florin Udrea is a professor in semiconductor engineering and head of the High Voltage Microelectronics and Sensors Laboratory at University of Cambridge. He received his B.Sc. from University of Bucharest, Romania in 1991, an M.Sc. in smart sensors from the University of Warwick, UK, in 1992 and the Ph.D. degree in power devices from the University of Cambridge, Cambridge, UK, in 1995. Since October 1998, Prof. Florin Udrea has been an academic with the Department of Engineering, University of Cambridge, UK. Between August 1998 and July 2003 he was an advanced EPSRC Research Fellow and prior to this, a College Fellow in Girton College, University of Cambridge. He is currently leading a research group in power semiconductor devices and solid-state sensors that has won an international reputation during the last 20 years. Prof. Udrea has published over 350 papers in journals and international conferences. He holds 70 patents with 20 more patent applications in power semiconductor devices and sensors. Prof. Florin Udrea co-founded three companies, Cambridge Semiconductor (Camsemi) in power ICs, Cambridge CMOS Sensors (CCS) in the field of smart sensors and Cambridge Microelectronics in Power Devices. Prof. Florin Udrea is a board director in Cambridge Enterprise. For his 'outstanding personal contribution to British Engineering' he has been awarded the Silver Medal from the Royal Academy of Engineering.

Andrea De Luca graduated from the University of Naples Federico II (Naples, Italy) with a degree in Electronic Engineering in 2011, and is currently a Ph.D. student at the University of Cambridge (Cambridge, UK). His research interests include temperature sensors, thermal flow sensors, infrared emitters and detector for non-dispersive-infrared spectroscopy, micro-hotplate based gas sensors and nanomaterials for infrared absorption/emission enhancement and gas sensing. He is author or co-author of 15 publications in journals and conferences, and co-inventor of one patent application.

Syed Zeeshan Ali graduated from GIK Institute (Pakistan) in 2003 with a B.S. in electronic engineering. He completed his Ph.D. in 2007 at the University of Cambridge (UK) on the design of micro-hotplates for smart gas sensors and electro-thermo-mechanical modeling of membrane devices and was then a research associate at the University of Cambridge researching on micro-hotplates and gas sensing materials. He joined Cambridge CMOS Sensors (UK) in 2010 and is at present an R&D Leader at the company. His areas of research are microsensors and MEMS devices including gas sensors, IR emitters and IR detectors. He is the author or co-author of over 50 publications in international journals and conferences.

Joan Ramon Morante received his Ph.D. from the University of Barcelona in 1980. Since 1985 he is full professor in the Department of Electronics. In 2008 he joined the Catalonia Institute of Research for Energy, IREC where he is the head of the Advanced Materials Area. His activities have been centered in electronic materials and devices; the assessment of their related technologies and production processes, specially emphasizing materials technology transfer. He is actively involved in research of new sensors, actuators and microsystems.